J|A|C|S COMMUNICATIONS

Published on Web 12/12/2008

Orthogonal Multi-Readout Identification of Alloy Nanowire Barcodes

U. Korcan Demirok,[†] Jared Burdick,[†] and Joseph Wang*[,‡]

The Biodesign Institute, Arizona State University, Tempe, Arizona 85287, Department of NanoEngineering, University of California San Diego, La Jolla, California 92093

Received August 12, 2008; E-mail: josephwang@ucsd.edu

The ability to prepare barcoded nanowires with a large variety of distinguishable patterns holds great promise for a wide range of tagging and identification applications.[1–3] Nanowires based on distinct striping,[1,4] compositional,[5] geometrical,[6] and magnetic[7,8] patterns have thus been developed and decoded by optical, electrochemical, or magnetic readout mechanisms.[1–3] While offering high coding capacity and distinct signatures, such nanowire barcodes and readout schemes commonly rely on a single level of identification. Multiple layers of information are desired for enhancing the protection and tracking of products and documents and hence for meeting major challenges associated with escalating counterfeiting criminal activity.

Here we present a multi-readout orthogonal detection of alloyed nanowires. The distinct characterization associated with the simultaneous use of several independent and powerful readout modes (based on different distinct processes and phenomena) and the resulting built-in redundancy make the new orthogonal strategy a unique and powerful tool in the armory of barcoded nanowires. Such integration of multiple readout mechanisms maximizes the available information and offers high confidence of identification compared to single readout systems. A judicious choice of the barcode composition and of the readout techniques is essential for the successful realization of such orthogonal identification of encoded nanomaterials.

The new orthogonal identification scheme has been demonstrated in connection to X-Ray fluorescence (XRF) as well as electrochemical and magnetic readouts of alloy nanowires (Scheme 1). Alloy nanowires have been shown to be extremely useful for generating a massive number of distinct compositionally encoded barcode patterns in connection to a single-step electrochemical preparation.[5] In designing alloy nanowires for the new orthogonal identification it is possible to enhance the identification power by codepositing different metal constituents for the various readout mechanisms. Ternary Ni−Zn−In alloy nanowires were selected here to provide distinct XRF (Ni−Zn), electrochemical (Zn−In), and magnetic (Ni) signatures.

For example, Figure 1 illustrates electrochemical (A) and XRF (B) signatures of the same Ni−Zn−In alloy nanowire barcodes. These nanowires were prepared by varying the concentration of Zn in the growth solution from 0.30 (a) to 0.24 (b) and to 0.18 M (c), while keeping the other metals (In and Ni) at a constant level (0.03 M). Both readout methods yield distinct patterns of two peaks of varying intensities. The resulting electrochemical signatures are characterized with Zn peaks (at −1.06 V) of decreasing current intensities, along with an In signal (at −0.59 V) of constant height (A). Similarly, the intensity of the XRF K-$L_{2,3}$ Zn emission peak (at 8.7 keV) correlates well with the Zn concentration in the plating solution, while the Ni emission peak (at 7.52 keV) remains constant (B).

Scheme 1. Orthogonal Identification of Alloyed Nanowire Barcodes[a]

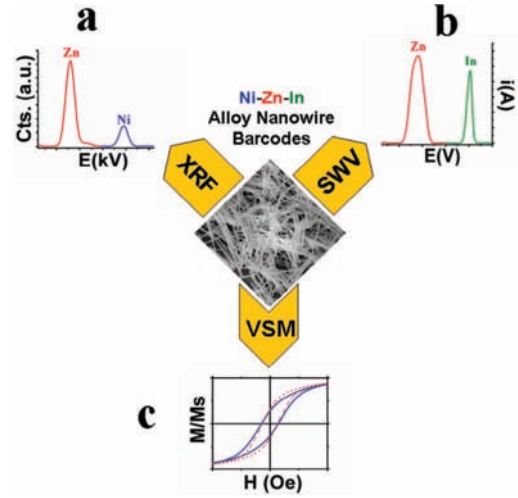

[a] The new multi-readout protocol is illustrated for XRF (a), square-wave voltammetric (SWV) (b), and vibrating sample magnetometric (VSM) (c) decoding of Ni−In−Zn ternary alloy nanowires. See text for details.

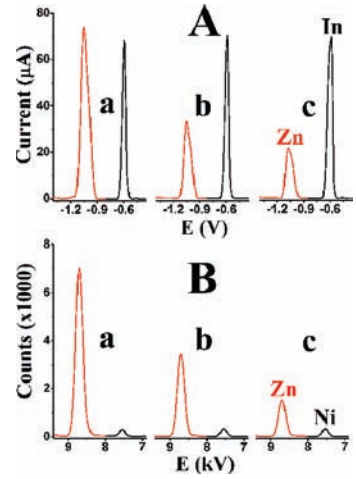

Figure 1. Electrochemical (A) and XRF (B) readouts of Zn−In−Ni alloyed nanowire barcodes grown from metal mixtures containing 0.03 M Ni and In along with 0.30 (a), 0.24 (b) and 0.18 M (c) Zn. See Supporting Information for experimental details.

The Ni component of the Ni−Zn−In alloy nanowires also provides a distinct magnetic coding that can be orthogonal to the XRF or electrochemical readouts to offer a third level of identification. For example, Figure 2 illustrates the simultaneous nondestructive XRF (a) and magnetic (b) readouts of two alloy nanowire samples. Both samples exhibited significantly different XRF and VSM profiles. The XRF signatures (top) are characterized with

[†] Arizona State University.
[‡] University of California San Diego.

10.1021/ja806396h CCC: $40.75

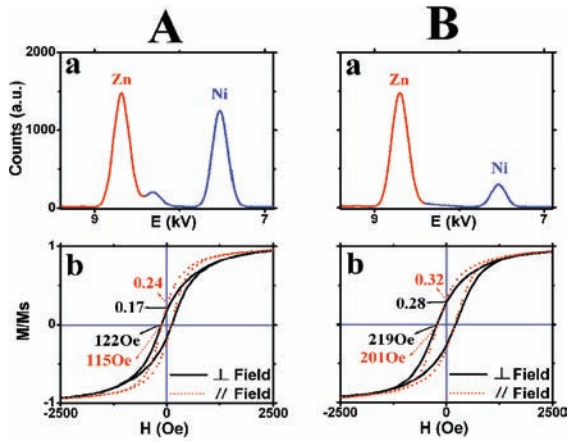

Figure 2. Simultaneous XRF (top row) and VSM (bottom row) readouts of Zn−In−Ni nanowires grown from solutions containing 180 mM Zn, 80 mM In, and 165 mM Ni (A) and 180 mM Zn, 30 mM In, and 30 mM Ni (B). See Supporting Information for experimental details.

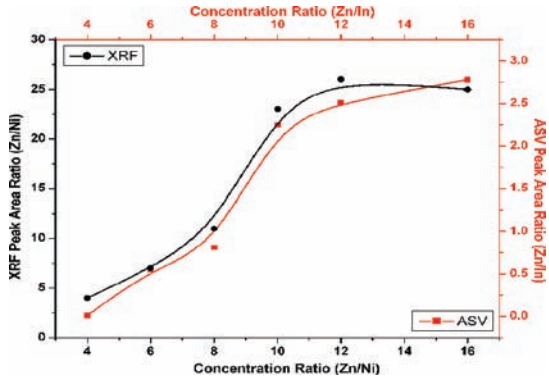

Figure 3. Dependence of the XRF Zn/In intensity ratio (●) and of the voltammetric Zn/In peak ratio (■) for alloy nanowires upon changing the concentration ratios of the corresponding metals in the growth solution. Concentration ratios of zinc to the corresponding metals were varied by changing the Zn concentration from 0.12 to 0.48 M while keeping the Ni and In levels at 0.03 M.

distinct Ni and Zn peaks, with the Ni signals reflecting the different Ni concentrations in the plating solutions [165 (A) and 30 mM (B)]. An additional K-M_3 Ni shoulder peak is observed around 8.4 kV using the nickel-rich alloy, providing additional decoding information (Figure 3A,a). Note also the similar intensity of the Zn peak (at 8.7 keV). Both nanowire samples exhibit well-defined distinguishable magnetic patterns, with hysteresis loops under a varying external magnetic field, common to magnetization−demagnetization of the local magnetic domains within the nanowires (bottom). Slight differences in the magnetic remanence and coercivity values are observed upon applying parallel and perpendicular magnetic fields with respect to the nanowire axis. Note that the remanence and coercivity values (under both parallel and perpendicular fields) decrease upon increasing the nickel content (B vs A). The smaller coercivity and remanence of the nickel-rich sample (A) can be attributed to the discontinuity and heterogeneity of the ferromagnetic domains formed during its electrodeposition.[9] Polycrystallinity, the shape of the nanowire ends, and variations in the wire diameter can also contribute to lower magnetic coercivity.[10,11]

In designing alloy nanowires for orthogonal detection it is important to understand the correlation between the composition of the growth solution and that of the resulting alloy nanowires. Figure 3 displays the dependence of the XRF Zn/In intensity ratio (●) and the voltammetric Zn/In peak ratio (■) upon the concentration ratios of the corresponding metals in the growth solution. For this purpose, the concentrations of In and Ni in the growth solution were fixed at 0.03 M while the level of Zn was varied from 0.12 M to 0.48 M. Despite the variances in the sensitivity of the XRF and electrochemical readouts toward the target metals, the two methods display similar sigmodial concentration−composition profiles. Such nonlinear profiles are characteristic of electrodeposited alloys, particularly those containing Zn and Ni,[12] and reflect the complex charge-transfer-coupled alloy deposition mechanism governing the deposition of individual metals from a common growth mixture solution. Such composition−concentration curves are extremely useful for selecting the most suitable concentration range for generating distinct multi-readout barcode signatures. Further (TEM/EDX) characterization of the elemental distribution and mapping is included in the Supporting Information.

In conclusion, we demonstrated that it is possible to combine multiple readout mechanisms of the same alloyed nanowires. Such coupling of multiple identification methods, offering different kinds of information, is unique among methods used for decoding barcoded nanomaterials. It maximizes the available information and offers great promise for enhancing the identification power of encoded nanostructures and hence for meeting the major challenges of product protection and tracking. The power of such multi-readout orthogonal detection can be further enhanced by developing new algorithms for data processing and fusion and by adding additional readout mechanisms. While the new concept has been presented in connection to orthogonal (XRF, electrochemical, magnetic) identification of alloy nanowires, it could be readily extended to other encoded nanomaterials and different readout mechanisms.

Acknowledgment. This work was supported by the National Science Foundation (Grant Number CHE 0506529).

Supporting Information Available: Experimental details and protocols. This material is available free of charge via the Internet at http://pubs.acs.org.

References

(1) Finkel, N. H.; Lou, X.; Wang, C.; He, L. *Anal. Chem.* **2004**, *76*, 352A–359A.
(2) Keating, C. D.; Natan, M. J. *Adv. Mater.* **2003**, *15*, 451–454.
(3) Bulbarello, A.; Sattayasamitsathit, S.; Crevillen, A. G.; Burdick, J.; Mannino, S.; Kanatharana, P.; Thavarungkul, P.; Escarpa, A.; Wang, J. *Small* **2008**, *4*, 597–600.
(4) Nicewarner-Pena, S.; Freeman, R.; Reiss, B. D.; He, L.; Pena, D.; Walton, I.; Cromer, R.; Keating, C. D.; Natan, M. J. *Science* **2001**, *294*, 137–141.
(5) Sattayasamitsathit, S.; Burdick, J.; Bash, R.; Kanatharana, P.; Thavarungkul, P.; Wang, J. *Anal. Chem.* **2007**, *79*, 7571–7575.
(6) Matthias, S.; Schilling, J.; Neilsch, K.; Müller, F.; Wehrspohn, R.; Gösele, U. *Adv. Mater.* **2002**, *14*, 1618–1621.
(7) Choi, J.; Oh, S. J.; Ju, H.; Cheon, J. *Nano Lett.* **2005**, *5*, 2179–2183.
(8) Lee, J. H.; Wu, J. H.; Liu, H. L.; Cho, J. U.; Cho, M. K.; An, B. H.; Min, J. H.; Noh, S. J.; Kim, Y. K. *Angew. Chem.* **2007**, *119*, 3737–3741.
(9) Kawai, S.; Ishiguro, I. *J. Electrochem. Soc.* **1976**, *123, 7*, 1047–1051.
(10) Yu, C. Y.; Yu, Y. L.; Sun, H. Y.; Xu, T.; Li, X. H.; Li, W.; Gao, Z. S.; Zhang, X. Y. *Mater. Lett.* **2007**, *61*, 1859–1862.
(11) Sellmyer, D. J.; Zheng, M.; Skomski, R. *J. Phys.: Condens. Matter* **2001**, *13*, R433–R460.
(12) Srimathi, S. N.; Mayanna, S. M.; Shesadri, B. S. *Surf. Technol.* **1982**, *16*, 277–322.

JA806396H